

Electrical power dissipation in semiconducting carbon nanotubes on single crystal quartz and amorphous SiO₂

Cheng-Lin Tsai,^{1,2} Albert Liao,^{3,4} Eric Pop,^{3,4,5} and Moonsub Shim^{1,2,a)}

¹Department of Materials Science and Engineering, University of Illinois, Urbana, Illinois 61801, USA

²Frederic Seitz Materials Research Laboratory, University of Illinois, Urbana, Illinois 61801, USA

³Department of Electrical and Computer Engineering, University of Illinois, Urbana, Illinois 61801, USA

⁴Micro and Nanotechnology Laboratory, University of Illinois, Urbana, Illinois 61801, USA

⁵Beckman Institute, University of Illinois, Urbana, Illinois 61801, USA

(Received 6 May 2011; accepted 15 July 2011; published online 5 August 2011)

Heat dissipation in electrically biased individual semiconducting carbon nanotubes (CNTs) on single crystal quartz and amorphous SiO₂ is examined with temperature profiles obtained by spatially resolved Raman spectroscopy. Despite the differences in phonon velocities, thermal conductivity, and van der Waals interactions with CNTs, on average, heat dissipation into single crystal quartz and amorphous SiO₂ is found to be similar. Large temperature gradients and local hot spots often observed underscore the complexity of CNT temperature profiles and may be accountable for the similarities observed. © 2011 American Institute of Physics. [doi:10.1063/1.3622769]

Exceptional electrical and thermal properties make carbon nanotubes (CNTs) excellent candidates for next-generation electronics including high performance transistors, electrical interconnects, heat sinks, and nanoscale heaters.^{1–3} With the aggressive down-scaling of device dimensions and increase in circuit density, thermal management becomes increasingly important. In addition to providing information about diameter/chirality and degree of disorder, Raman-active phonon modes can furnish insights into the thermal response of CNTs.^{4–6} Because of the importance of optical phonon (OP) scattering at high biases, Raman studies have been valuable in understanding non-equilibrium electron transport in both CNTs and graphene.^{5,7,8} For instance, hot OPs as well as CNT-substrate interactions strongly influence high-field electron transport characteristics (e.g., negative differential conductance being observed only in suspended CNTs rather than those resting on an SiO₂ substrate⁹). Hence, examining how different substrates influence thermal response is essential for the design of CNT electronics.

Amorphous SiO₂ (a-SiO₂) as a thermally grown oxide on heavily doped Si is by far the most common CNT substrate used to date. However, single-crystal quartz has also become important as it can lead to nearly perfect alignment of CNTs during growth.¹⁰ The two substrates have the same constituent atoms, but substantially different thermal conductivities. Furthermore, spontaneous alignment on single crystal quartz has been attributed to strong van der Waals (vdW) interactions along the growth direction,¹¹ which should, in principle, result in better thermal coupling. These differences and similarities have motivated this study on comparing heat dissipation processes in electrically biased semiconducting CNTs on these two substrates. Furthermore, while temperature profiles of metallic CNTs supported on substrates or suspended have been previously examined,^{12,13} similar spatially resolved studies have not been reported on semiconducting CNTs. Non-uniform electric fields expected and sensitivity to local chemical environment especially to substrate surface charges make it

even more important for such studies to be carried out on devices incorporating semiconducting CNTs.

Horizontally aligned CNTs were grown by chemical vapor deposition on ST-cut quartz (Hoffman Materials) using ferritin (Sigma-Aldrich) and CH₄ as the catalyst and carbon source, respectively.¹⁴ For measurements on a-SiO₂ substrates, aligned CNTs grown on quartz were transferred onto Si substrates with thermal oxide (300 nm).¹⁵ Lithographically patterned metal electrodes (2 nm Ti and 50 nm Pd) were deposited to define 4 μm long CNT channels. Scanning electron microscopy (SEM), atomic force microscopy (AFM), and electrical breakdown¹⁶ were conducted to determine length, diameter, and location of failure as well as to ensure that only one CNT spanned the channel of interest. Raman measurements were carried out on Jobin-Yvon Labram HR800 using a 100 × air objective with 633 nm laser excitation source and Ar flowing over the samples. The laser spot size was ~1 μm and the power was kept at 1 mW.

Figure 1 shows Raman G-band spectra of a semiconducting CNT on quartz under electrical bias (V_d). The downshift of the G-band frequency (ω_G) with increasing V_d indicates increasing temperature (T) from Joule heating. Due to the higher intensity, we consider only the longitudinal optical phonon mode here. Estimates of T from changes in ω_G are often made using the calibrated Raman G-band T coefficient, $\chi_G \sim -0.03 \text{ cm}^{-1}/\text{K}$.^{14,17,18} However, such calibrations are made under equilibrium conditions. Joule heating leads to a non-equilibrium situation where charge carriers and OPs are at a significantly higher T than the lattice.^{5,7,8} Therefore, to estimate the lattice T , we utilize $d\omega_G/dT_{\text{RBM}} = -0.021 \text{ cm}^{-1}/\text{K}$ given in Ref. 5 where the ω_G downshift with Joule heating was reported along with the temperature of the radial breathing mode (which should be at equilibrium with the lattice).

Figure 1(b) shows the change in ω_G and the corresponding change in T as a function of power per unit length (P). If we simply approximate T profile as being uniform along the length (x) of a 4 μm long CNT, we expect $T(x) = T_o + P/g$, where T_o is the substrate T and g is the thermal conductance

^{a)}Electronic mail: mshim@illinois.edu.

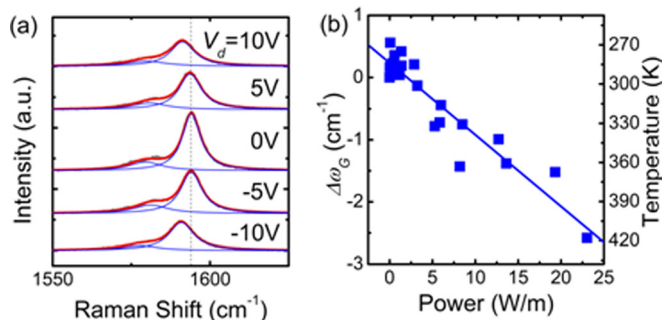


FIG. 1. (Color online) (a) G-band Raman spectra of a 4 μm long semiconducting CNT on quartz at the indicated source-drain bias (V_d). (b) Change in G-band frequency ($\Delta\omega_G$) and the corresponding temperature as a function of power per unit length. Solid line is a linear fit.

per unit length from the CNT.¹⁹ Here, g includes the interfacial CNT-substrate thermal resistance in series with a spreading heat conduction term into the substrate; however, the former typically dominates.¹⁶ From the linear fit shown in Fig. 1(b), we obtain $g = 0.18 \text{ Wm}^{-1}\text{K}^{-1}$, similar to previously reported values.^{5,19,20} However, an asymmetric T profile with the highest T near the ground electrode (assuming hole transport with positive V_d) is expected in semiconducting CNTs due to the non-uniform electric field along their length.²¹ Electrical breakdown measurements have recently demonstrated that this is indeed, on average, the exhibited behavior.¹⁶ These expectations and findings point to the importance of direct measurements of T profiles during Joule heating of semiconducting CNT devices.

An asymmetric profile with T drop as large as $\sim 550 \text{ K}$ around the midpoint with the highest T occurring near the ground electrode can be seen for a semiconducting CNT on a-SiO₂ substrate in Fig. 2(a). When the polarity of the applied V_d is reversed, the maximum T position shifts accordingly, indicating that the observed behavior is not an artifact of asymmetric contact resistance.²² The SEM image taken after all measurements have been carried out, and V_d pushed to device failure shows the location of electrical breakdown to be at the expected position of highest T . Figure 2(b) shows that T measurements made at only one location can lead to large apparent variations in g : the highest T location yields $g = 0.07 \text{ Wm}^{-1}\text{K}^{-1}$ versus $0.14 \text{ Wm}^{-1}\text{K}^{-1}$ at $1.5 \mu\text{m}$ from the left electrode. Similarly, large discrepancies are shown in Figs. 2 for a semiconducting CNT on quartz with $g = 0.06 \text{ Wm}^{-1}\text{K}^{-1}$ and $0.18 \text{ Wm}^{-1}\text{K}^{-1}$ near and away from the highest T region, respectively.

While 16 out of 24 semiconducting CNTs examined exhibit T profiles similar to those shown in Fig. 2 with the highest T location closer to the ground electrode (Fig. 3 inset), a significant number of CNTs show what appears to be a random distribution of local hot spots. Examples are shown in Fig. 3 and in the supplementary material. These results further emphasize the importance of obtaining T profiles and the necessity of a better approach to extracting g values in order to compare different substrates. Following Ref. 16, we solve the heat diffusion equation along the CNT using two distinct power dissipation profiles $P(x)$ to capture the two types of behaviors. A quadratic $P(x)$ is used for behavior of the type in Fig. 2. A Gaussian with a constant background is used for cases similar to Fig. 3. Solid lines in Figs. 2 and 3 are the fitted T profiles, and Fig. 4 shows the extracted g val-

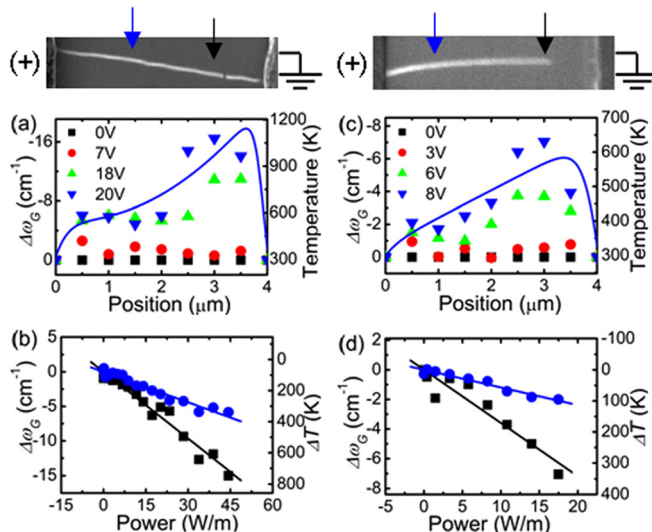


FIG. 2. (Color online) Temperature profiles from measured G-band frequency shift ($\Delta\omega_G$) at the indicated voltages and corresponding SEM images taken after electrical breakdown for a CNT on quartz (a) and on a-SiO₂ (c) substrates. Solid curves for the highest bias cases are the fitted temperature profiles. Power dependence of G-band frequency shift and the corresponding temperature change at the locations indicated by the arrows in the SEM images for the same CNTs on quartz (b) and a-SiO₂ (d). Filled squares (circles) correspond to right (left) arrow locations. Solid lines are linear fits.

ues. We note that the Gaussian profile captures the experimental results better whenever there is a steep T gradient even if the CNT exhibits expected maximum T near the ground electrode. This behavior may indicate that significant number of otherwise “well-behaved” semiconducting CNTs may nevertheless fall within the category with random local hot spots. In fact, more than half of CNTs examined (13 out of 24) are better described as having local hot spots.

To consider how the two different substrates should affect heat dissipation, we compare our results to the diffuse mismatch model (DMM)²³ in Fig. 4. We calculate $g(T)$ using DMM following Ref. 16 for a 1.5 nm diameter CNT (all CNTs examined here have diameter between 1 and 2 nm as measured by AFM). The values shown include the heat spreading thermal resistance into the substrates. While DMM provides only upper limits, quartz is predicted to exhibit better thermal coupling than a-SiO₂ as shown in Fig. 4. This may be expected since quartz has higher phonon velocity, thermal conductivity, and atomic density. Given that CNTs should have stronger vdW interactions with quartz

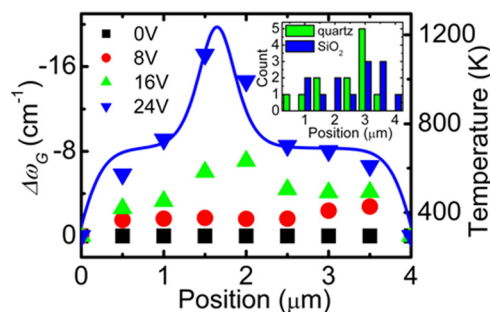


FIG. 3. (Color online) Temperature profiles at the indicated electrical bias (ground electrode on the right side) for a CNT showing an unexpected heating behavior. Solid curve is the fitted profile from solving the heat diffusion (Ref. 16) equation using a Gaussian power profile. Histogram of the highest T locations for all CNTs examined is shown in the inset.

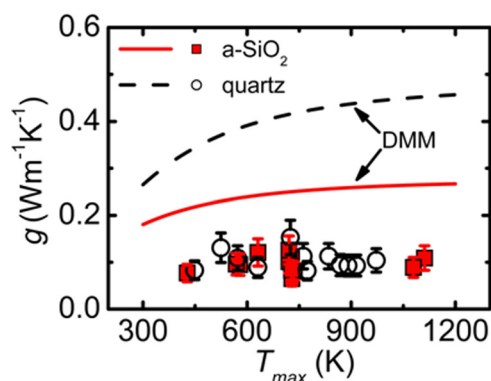


FIG. 4. (Color online) Comparison of experimental (symbols) and calculated (lines) values of thermal conductance including heat spreading into the substrates (g) on quartz (circles) and a-SiO₂ (squares). T_{max} is the maximum temperature experimentally measured. Error bars reflect $\pm 0.005 \text{ cm}^{-1}/\text{K}$ uncertainty in G-band T coefficient often reported (see Ref. 14).

(along the alignment direction)¹¹ than with a-SiO₂, an even larger difference in interfacial thermal coupling could be expected based on recent molecular dynamics simulations.²⁴ Surprisingly, we observe no difference between quartz and a-SiO₂ substrates in Fig. 4 within experimental error margins (average $g = 0.10 \pm 0.02 \text{ Wm}^{-1}\text{K}^{-1}$ is obtained with each substrate for this range of CNT diameters).

There are several mechanisms which may be consistent with the similar thermal coupling observed. Surface phonon polariton (SPP) scattering was theoretically suggested to be an important energy dissipation pathway.²⁵ Quartz and a-SiO₂ should have similar SPPs, which would then lead to similar thermal coupling. In fact, calculations based on quartz have been used to describe CNT devices on a-SiO₂ substrates.²⁶ However, the SPP mechanism should be sensitive to the vdW distance, and stronger vdW interactions expected on quartz¹¹ should lead to better thermal coupling. Furthermore, local hot spots we observe cannot be explained by the SPP mechanism. Even the more common cases, where the maximum T occurs near the ground electrode, are often better described by Gaussian profiles suggesting that these may also be random local hot spots that happen to be near the ground electrode.²²

Adsorbed molecules such as hydrocarbons, water, and oxygen from the ambient may provide alternate and parallel heat dissipation pathways.²⁷ Given the same ambient gas environment, possible molecular pathways should be similar for the two substrates and such a mechanism would be consistent with local hot spots, i.e., random distributions of adsorbed molecules. However, at least for hydrocarbons and surfactants, thermal coupling between CNTs and “soft” molecules has been shown to be quite poor,^{28,29} and, based on our measured values of g , direct coupling to the substrate should be about an order of magnitude better.

Charge trapping in the substrate surface may also play an important role. Substrate charging has been shown to cause large hysteresis in CNT transistors,^{30,31} and such charges can lead to large local electric fields that may be responsible for the observed local hot spots. Localized substrate charging may even introduce electrostatic forces that can strongly alter local interactions (e.g., a trapped hole would repel net positively charged p-type CNT). Such a scenario is consistent with random locations undergoing high degree of local heating leading to similar behavior on the two substrates.

Finally, we comment on the possible role of defects on the heat dissipation process. All CNTs examined here exhibit very little or no observable D-band in their Raman spectra. Intentional introduction of defects by covalent sidewall functionalization with 4-bromobenzene diazonium tetrafluoroborate does not significantly alter the heating behavior. This result can be explained by the “healing” effect of Joule heating as evidenced by the loss of the D-band upon electrical biasing.²²

In summary, we have shown that single crystal quartz and a-SiO₂ substrates exhibit similar thermal coupling to semiconducting CNTs. A significant number of CNTs exhibit unexpected local T spikes that may be explained by substrate surface charges leading to large local electric fields and possibly altering the local interactions. Understanding such unexpected heating behavior is especially important in devising efficient thermal management schemes for nanoscale devices.

This material is based upon work supported in part by the MSD Focus Center, under the Focus Center Research Program (FCRP), a Semiconductor Research Corporation entity, and in part by the NSF grants 09-05175 and CAREER 09-54423. Experiments were carried out in part in the Frederick Seitz Materials Research Laboratory Central Facilities, University of Illinois.

- ¹P. Avouris, Z. Chen, and V. Perebeinos, *Nat. Nanotechnol.* **2**, 605 (2007).
- ²J. Robertson, *Mater. Today* **10**, 36 (2007).
- ³F. Xiong, A. Liao, and E. Pop, *Appl. Phys. Lett.* **95**, 243103 (2009).
- ⁴Z. Yu and L. E. Brus, *J. Phys. Chem. A*, **104**, 10995 (2000).
- ⁵M. Steiner *et al.*, *Nat. Nanotechnol.* **4**, 320 (2009).
- ⁶T.-K. Hsu *et al.*, *J. Appl. Phys.* **108**, 084307 (2010).
- ⁷M. Oron-Carl and R. Krupke, *Phys. Rev. Lett.* **100**, 127401 (2008).
- ⁸S. Berciaud *et al.*, *Phys. Rev. Lett.* **104**, 227401 (2010).
- ⁹E. Pop, D. Mann, J. Cao, Q. Wang, K. Goodson, and H. Dai, *Phys. Rev. Lett.* **95**, 155505 (2005).
- ¹⁰S. J. Kang, C. Kocabas, T. Ozel, M. Shim, N. Pimparkar, A. Alam, S. V. Rotkin, and J. A. Rogers, *Nat. Nanotechnol.* **2**, 230 (2007).
- ¹¹J. Xiao, S. Dunham, P. Liu, Y. Zhang, C. Kocabas, L. Moh, Y. Huang, K.-C. Hwang, C. Lu, W. Huang, and J. A. Rogers, *Nano Lett.* **9**, 4311 (2009).
- ¹²V. V. Deshpande, S. Hsieh, A. W. Bushmaker, M. Bockrath, and S. B. Cronin, *Phys. Rev. Lett.* **102**, 105501 (2009).
- ¹³L. Shi *et al.*, *J. Appl. Phys.* **105**, 104306 (2009).
- ¹⁴T. Ozel, D. Abdula, E. Hwang, and M. Shim, *ACS Nano* **3**, 2217 (2009).
- ¹⁵S. J. Kang *et al.*, and J. A. Rogers, *Nano Lett.* **7**, 3343 (2007).
- ¹⁶A. Liao, R. Alizadegan, Z.-Y. Ong, S. Dutta, F. Xiong, K. J. Hsia, and E. Pop, *Phys. Rev. B*, **82**, 205406 (2010).
- ¹⁷H. D. Li, K. T. Yue, Z. L. Lian, Y. Zhan, L. X. Zhou, S. L. Zhang, Z. J. Shi, Z. N. Gu, B. B. Liu, R. S. Yang, H. B. Yang, G. T. Zou, Y. Zhang, and S. Iijima, *Appl. Phys. Lett.* **76**, 2053 (2000).
- ¹⁸Y. Zhang *et al.*, *J. Phys. Chem. C* **111**, 14031 (2007).
- ¹⁹E. Pop, *Nanotechnology* **19**, 295202 (2008).
- ²⁰H. Maune, H.-Y. Chiu, and M. Bockrath, *Appl. Phys. Lett.* **89**, 013109 (2006).
- ²¹Y. Ouyang and J. Guo, *Appl. Phys. Lett.* **89**, 183122 (2006).
- ²²See supplementary material at <http://dx.doi.org/10.1063/1.3622769> for figures showing effects of reversing bias polarity, additional examples of local hot spots in T profiles, annealing defects at high bias, and parameters used in DMM model.
- ²³E. T. Swartz and R. O. Pohl, *Rev. Mod. Phys.* **61**, 605 (1989).
- ²⁴Z.-Y. Ong and E. Pop, *Phys. Rev. B* **8**, 155408 (2010).
- ²⁵S. Rotkin *et al.*, *Nano Lett.* **9**, 1850 (2009).
- ²⁶A. G. Petrov and S. V. Rotkin, *JETP Lett.* **84**, 156 (2006).
- ²⁷D. Mann *et al.*, *J. Phys. Chem. B* **110**, 1502 (2006).
- ²⁸S. T. Huxtable, D. G. Cahill, S. Shenogin, L. Xue, R. Ozisik, P. Barone, M. Usrey, M. S. Strano, G. Siddons, M. Shim, and P. Keblinski, *Nature Mater.* **2**, 731 (2003).
- ²⁹S. Shenogin, L. Xue, R. Ozisik, P. Keblinski, and D. G. Cahill, *J. Appl. Phys.* **95**, 8136 (2004).
- ³⁰W. Kim, A. Javey, O. Vermesh, Q. Wang, Y. Li, and H. Dai, *Nano Lett.* **3**, 193 (2003).
- ³¹D. Estrada *et al.*, *Nanotechnology* **21**, 085702 (2010).

SUPPLEMENTAL INFORMATION FOR

Electrical power dissipation in carbon nanotubes on single crystal quartz and amorphous SiO₂

Cheng-Lin Tsai,^{1,2} Albert Liao,^{3,4} Eric Pop,^{3,4,5} and Moonsub Shim^{1,2}

¹*Dept. of Materials Science & Engineering, Univ. of Illinois, Urbana, Illinois 61801, USA*

²*Frederic Seitz Materials Research Laboratory, Univ. of Illinois, Urbana, Illinois 61801, USA*

³*Dept. of Electrical & Computer Engineering, Univ. of Illinois, Urbana, Illinois 61801, USA*

⁴*Micro and Nanotechnology Laboratory, Univ. of Illinois, Urbana, Illinois 61801, USA*

⁵*Beckman Institute, University of Illinois, Urbana, Illinois 61801, USA*

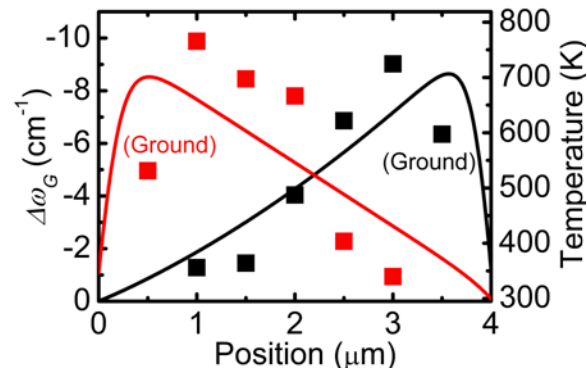


FIG. S1. Comparison of temperature profile of a CNT under Joule heating before and after the voltage polarity is reversed ($|V_d| = 15$ V). The ground electrode is indicated for both cases. Solid curves are fitted temperature profiles from solving the heat diffusion equation along the CNT quadratic power profiles, $P(x)$ (see Ref. 1)

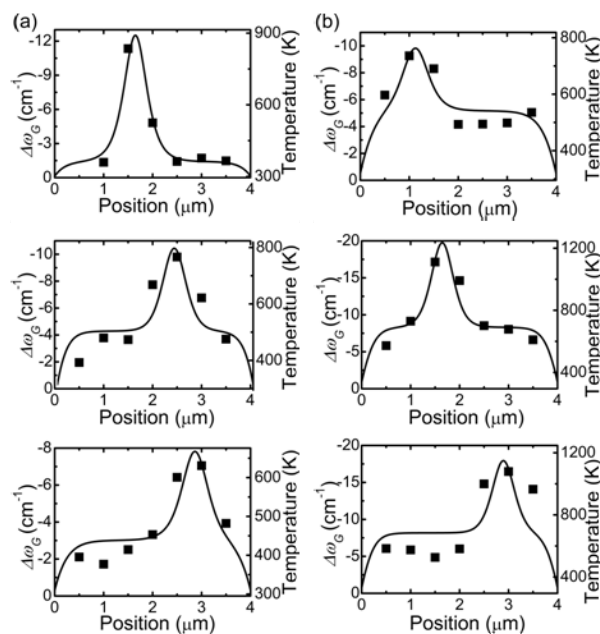


FIG. S2. Random temperature spikes on (a) quartz and (b) amorphous SiO_2 (a- SiO_2) substrates. Solid curves are fitted temperature profiles from solving the heat diffusion equation using Gaussian power profiles (see Ref. 1). In all cases, the ground electrode is at position = 4 μm . Even the expected maximum temperature near the ground electrode for positively biased p-type carbon nanotubes (as seen in bottom two data sets) are often better described by Gaussian power profiles, underlining the importance of obtaining temperature profiles and the unexpected local hot spots that may dictate heat dissipation processes.

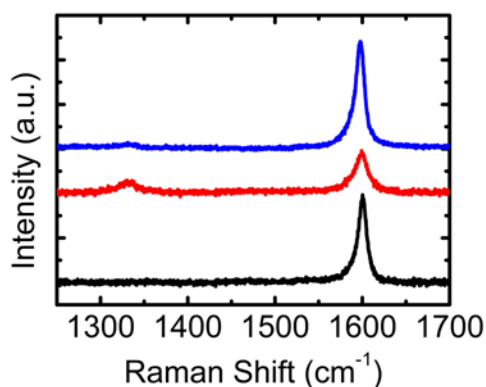


FIG. S3. (a) Raman spectra of a CNT before 4-bromobenzene diazonium tetrafluoroborate (4-BBDT) functionalization (black), after 1mM 4-BBDT functionalization (red), (Ref. 2) and after $V_d = 16$ V is applied (blue) demonstrating the disappearance of the D-band ~ 1320 cm^{-1} and therefore the “healing” effects upon Joule heating.

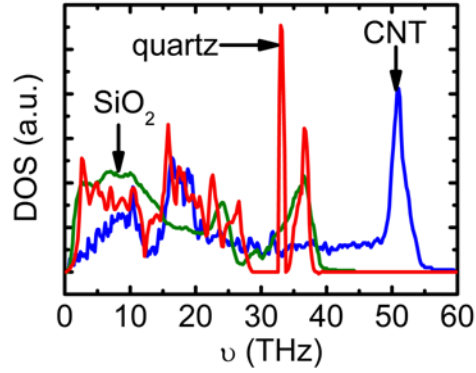


FIG. S4. Phonon density of states (DOS) of a CNT, a-SiO₂, and quartz used in the diffuse mismatch model (DMM) calculations. Phonon DOS are from Ref. 1 for the CNT and a-SiO₂ and Ref. 3 below for quartz.

Table I. Parameters used in the DMM model.

Parameter	a-SiO ₂	Quartz
v_{CNT}	932 m/s	932 m/s
v_{ox}	4.1 km/s (Ref. 4)	5 km/s (Ref. 5)
N_{CNT}	16.3 atoms/Å	16.3 atoms/Å
N_{ox}	0.0227 molecules/Å ³	0.0273 molecules/Å ³
d	1.5 nm	1.5 nm

v = phonon velocity, N = atomic/molecular density, d = diameter. *CNT* refers to carbon nanotube and *ox* refers to oxide substrates. v_{ox} for quartz given is the average of [001] and [100] directions. v_{CNT} is the average of longitudinal and transverse modes in graphite, perpendicular to the graphitic planes (c-axis). (Ref. 6)

The total interfacial thermal boundary conductance, g , includes the effect of heat spreading into the oxide substrate, g_{ox} , as given in Ref. 1 below. To calculate g_{ox} , thermal conductivity of 1.4 Wm⁻¹K⁻¹ for a-SiO₂ (Ref. 7) and 10.2 Wm⁻¹K⁻¹ (average of [001] and [010] directions) for quartz (Ref. 8) are used.

Supplementary References

- ¹ A. Liao, R. Alizadegan, Z.-Y. Ong, S. Dutta, F. Xiong, K. J. Hsia, and E. Pop, Phys Rev. B, **82**, 205406 (2010).
- ² K.T. Nguyen and M. Shim, J. Am. Chem. Soc. **131**, 7103 (2009).
- ³ A. N. Kislov, M. O. Toropov, and A. F. Zatspein, Journal of Non-Crystalline Solids, **357**, 1912 (2011).
- ⁴ P. G. Sverdrup, Y. S. Ju, and K. E. Goodson, J. Heat Transfer, **123**, 130 (2001).
- ⁵ M. Höfer, F. R. Schilling, Phys. Chem. Minerals, **29**, 571 (2002).
- ⁶ K. Sun, M. A. Stroscio, and M. Dutta, Superlattices Microstruct. **45**, 60 (2009).
- ⁷ D. G. Cahill, M. Katiyar, and J. R. Abelson, Phys. Rev. B, **50**, 6077 (1994).
- ⁸ H. Kanamori, N. Fujii, and H. Mizutani, Journal of Geophysical Research, **73**, 595 (1968).